

# Continuous Dynamic Bipedal Jumping via Adaptive-model Optimization

Junheng Li, Omar Kolt, and Quan Nguyen

**Abstract**—Dynamic and continuous jumping remains an open yet challenging problem in bipedal robot control. The choice of dynamic models in trajectory optimization (TO) problems plays a huge role in trajectory accuracy and computation efficiency, which normally cannot be ensured simultaneously. In this letter, we propose a novel adaptive-model optimization approach, a unified framework of Adaptive-model TO and Adaptive-frequency Model Predictive Control (MPC), to effectively realize continuous and robust jumping on HECTOR bipedal robot. The proposed Adaptive-model TO fuses adaptive-fidelity dynamics modeling of bipedal jumping motion for model fidelity necessities in different jumping phases to ensure trajectory accuracy and computation efficiency. In addition, conventional approaches have unsynchronized sampling frequencies in TO and real-time control, causing the framework to have mismatched modeling resolutions. We adapt MPC sampling frequency based on TO trajectory resolution in different phases for effective trajectory tracking. In hardware experiments, we have demonstrated robust and dynamic jumps covering a distance of up to 40 cm (57% of robot height). To verify the repeatability of this experiment, we run 53 jumping experiments and achieve 90% success rate. In continuous jumps, we demonstrate continuous bipedal jumping with terrain height perturbations (up to 5 cm) and discontinuities (up to 20 cm gap).

## I. INTRODUCTION

Bipedal robots have demonstrated a large step of advancement in dynamic, adaptive, and robust locomotion in recent years [1], [2], [3], [4], [5]. Traditional approaches in bipedal locomotion control rely on periodic walking gait to ensure stability and always in-contact [6], [7]. Boston Dynamics and Unitree Robotics have showcased impressive parkour and back-flipping motions on full-size humanoid robots [8], [9], demonstrating the capability of bipedal/humanoid robots in locomotion techniques with extended flight phases and beyond walking gaits. With the motivation of allowing bipedal robots to robustly traverse challenging and discontinuous terrains with adaptivity and agility like humans, in this work, we focus on developing a robust and versatile bipedal jumping control framework.

Jumping motion planning and control on quadruped robots have been extensively studied by many research groups in the past years. Many model-based control approaches involve solving offline trajectory optimization (TO) problems. For instance, Nguyen et al. proposed 2D jumping TO with a full quadruped dynamics model [10]. Chignoli et al. used Kino-dynamic TO with a jump feasibility classifier for rapid generation of jumping trajectories [11]. Ding et al. formulated

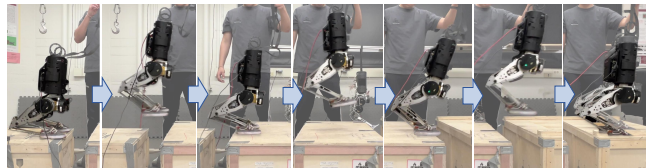


Fig. 1: Continuous Jumping over Discrete Terrain on HECTOR Bipedal Robot. Full Supplementary Video: <https://youtu.be/EQFgdbFYKvs>

the jumping problem into a mix-integer convex programming problem with centroidal dynamics [12]. Bellegarda et al. realized rapid online jumping planning by parameterizing foot force profiles [13].

Due to the inherently unstable and under-actuated nature of bipedal robots, bipedal jumping consists of more challenges in model-based control system design, such as in addressing (1) leveraging whole-body motion for takeoff, (2) effective pose tracking during the flight phase for optimal landing configuration, (3) impact mitigation upon landing, (4) robust balancing after impact, and (5) transferability to hardware. Related works have made attempts to address these challenges partially. For instance, Chignoli et al. realized dynamic 3D acrobatic behaviors numerically on the MIT humanoid via actuation-aware Kino-dynamic TO. [14]. Wensing et al. proposed a Prioritized Task-Space Control for generating humanoid jumping behaviors online [15]. Xiong et al. developed a spring-mass model for bipedal hopping with a control-Lyapunov-function-based quadratic program [16]. Zhang et al. proposed a heuristic landing control to ensure stability after landing [17]. Yang et al. leveraged impact invariant control for robust bipedal landing [18].

It is noticed that many related works choose to employ only a single dynamics model in TO. This modeling choice of a jumping TO problem in current frameworks faces two extremes. On one hand, Kino-dynamic TO assumes the robot as a single-rigid-body dynamics (SRBD) model or centroidal dynamics model [19] with kinematic constraints [20], which sacrifices model accuracy for very efficient computation and conflicts with the dynamic effects of all links in whole-body jumping motions. On the other hand, whole-body dynamics TO utilizes a full-order Euler-Lagrangian dynamics model of the robot and contact dynamics for very accurate trajectory planning but may require extended time for solutions [21]. In the author's prior work, the full-order dynamics model of a quadruped robot (3-DoF legs, 18 DoF total) is used, which requires up to 15 minutes to generate one 3-D dynamic motion trajectory in MATLAB [22]. Applying this approach to bipedal robots with 5-DoF legs will induce even more

Junheng Li, Omar Kolt, and Quan Nguyen are with the Department of Aerospace and Mechanical Engineering, University of Southern California, Los Angeles, CA 90089.

Corresponding Author: Junheng Li, [junheng1@usc.edu](mailto:junheng1@usc.edu).

This work is supported by USC Departmental Startup Fund.

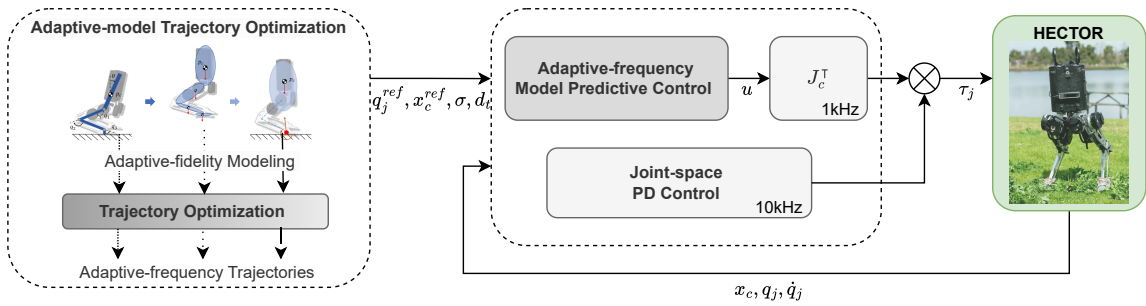


Fig. 2: System Architecture

computation burden. In this work, we attempt to address the above problems altogether by finding a well-balanced middle ground and proposing an adaptive-model TO framework that takes into consideration the model fidelity requirement in TO during different jumping phases to balance the resolution of the trajectory and computation effort. The proposed framework can generate accurate and hardware-realizable trajectories and keep the computation time in a few seconds.

Allowing adaptivity of the modeling in optimization problems has become a popular strategy in model-based control. Recently, hierarchical-model-based approaches become popular online control approaches. Li et al. proposed Model Hierarchical Predictive Control that prioritizes high-resolution models in near MPC horizons and uses reduced-order models in far prediction horizons [23], [24]. Csomay-Shanklin et al. designed the geometric MPC prediction horizon to have a fine sampling rate during contact and a relaxed sampling rate during the flight phase on monoped robots. [25].

Conventional model-based tracking control strategies use fixed-frequency control that is unsynchronized with optimal trajectories (e.g., [22], [14]), which does not fully leverage the model resolution for effective tracking performance. In this work, we leverage adaptive modeling in TO and design real-time tracking and balancing control with only an SRBD-based adaptive-frequency MPC [26] to synchronize with TO frequency. Compared to traditional jumping TO frameworks, we design the bipedal jumping TO to consist of (1) adaptive dynamics models, for balancing computation effort and model resolution at different jumping phases, (2) adaptive sampling frequency, to synergize sampling rates with adaptive-frequency MPC, and (3) a SRBD-based recovery trajectory after landing, to synergize with MPC.

The main contributions of the letter are as follows:

- We develop a novel Adaptive-model Trajectory Optimization (TO) approach for bipedal jumping motion generation.
- To address the model resolution requirements at different stages of a jumping problem while minimizing computation effort, the proposed Adaptive-model TO incorporates 3 representations of bipedal dynamics models and sampling frequencies with varied orders of fidelity at takeoff, flight, and landing phases of a jumping motion. The models include 3-link inverted pendulum dynamics, multi-rigid-body dynamics (MRBD),

and single-rigid-body dynamics (SRBD).

- Hardware experimental validations have been conducted. We have realized HECTOR biped to jump over 40 cm in distance (57% of robot's height) in single jumps. We have also demonstrated the disturbance resistance of the proposed framework, including introducing up to 20 cm height perturbation in forward jumping.
- We have demonstrated continuous jumping over boxes with gaps of 20 cm. To our knowledge, we successfully showcase the first instance, in academic work, of dynamic continuous bipedal jumping on hardware over discrete terrains.
- Experiment repeatability with the proposed framework has been validated with a 90% success rate, based on 53 single bipedal jumps with varied jumping trajectories.

The rest of the paper is organized as follows. Section. II presents the overview of the proposed control system architecture. Section.III introduces the details of the bipedal robot models used in Adaptive-model Optimization, the nonlinear programming (NLP) problem definition of the Adaptive-model TO, and the Adaptive-frequency MPC. Section. IV presents the experimental validations.

## II. SYSTEM OVERVIEW

In this section, we introduce the system architecture of the proposed control architecture, shown in Fig. 2. The proposed Adaptive-model Optimization framework consists of two major parts, the Adaptive-model TO and the Adaptive-frequency MPC.

Conventional whole-body dynamics TO with contact induces a large computation burden, especially for bipedal robots with high-DoF legs, while reduced-order approaches, such as kino-dynamic TO, trade model fidelity for highly efficient motion generation. To effectively address the model resolution requirements during different phases of a bipedal jumping problem while balancing computation effort, the Adaptive-model TO leverages adaptive dynamics models and adaptive sampling rates to efficiently generate hardware-realizable jumping trajectories. With  $N$  time-steps, these trajectories are in terms of 2D reference trunk Center of Mass (CoM) states,  $x_c^{ref}$ , reference joint trajectories,  $q_{ip}^{ref}$ , contact sequence  $\sigma$ , and optimal sampling rates for takeoff, flight, and landing phases,  $dt^t$ ,  $dt^f$ , and  $dt^l$ . These trajectories are converted to 3D,  $x_c^{ref}$ ,  $q_j^{ref}$ , for real-time tracking control.

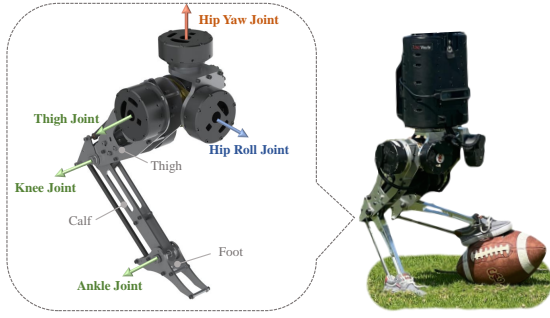


Fig. 3: HECTOR Biped and Leg Configuration.

When TO and real-time MPC operate at unsynchronized frequencies, conflicts can arise, as the finer-sampled optimized trajectory differs from the trajectory within the MPC prediction horizon due to varied step lengths. Hence, we pair the Adaptive-frequency TO with an Adaptive-frequency MPC. The MPC operates at adaptive sampling frequencies based on the TO at various phases of the jump. It works with joint-space PD controller together throughout the jumping motion and tracks the jumping trajectories. The resulting joint torques,  $\tau_j$ , from controllers are sent to the robot motors. The feedback states from the robot includes CoM states,  $\mathbf{x}_c = [\mathbf{p}_c; \Theta; \dot{\mathbf{p}}_c; \omega]$  and joint states,  $\mathbf{q}_j \in \mathbb{R}^{10}$ ,  $\dot{\mathbf{q}}_j \in \mathbb{R}^{10}$ . Where  $\mathbf{p}_c \in \mathbb{R}^3$  is trunk CoM location,  $\Theta \in \mathbb{R}^3$  represents robot's Euler angles,  $\Theta = [\phi; \theta; \psi]$ ,  $\dot{\mathbf{p}}_c \in \mathbb{R}^3$  is trunk CoM velocity,  $\omega \in \mathbb{R}^3$  is the world frame angular velocity.

### III. PROPOSED APPROACH

In this section, we introduce the proposed approaches in this work, including the choice of adaptive dynamics models of the bipedal robot jumping problem, formulation of Adaptive-model TO, and Adaptive-frequency MPC.

#### A. HECTOR Bipedal Robot

The bipedal robot used in this work is the HECTOR robot. HECTOR, introduced in the author's prior work [27], stands for Humanoid for Enhanced ConTrol and Open-source Research. The open-source simulation frameworks of HECTOR project can be found in [28]. HECTOR biped consists of 5-DoF legs with ankle actuation, shown in Fig. 3. Standing at 70 cm and weighing 14 kg, the biped is actuated by Unitree A1 motors with 33.5 Nm of max torque and 21.0 rad/s max joint speed. The knee joint is designed to have a gear ratio of 2:1 w.r.t. the knee motor, which doubles the joint torque at the knee to 67.0 Nm. Detailed physical parameters are outlined in [27].

HECTOR's full joint-space Euler-Lagrangian dynamics equation of motion is described as follows. The joint-space generalized states  $\mathbf{q} \in \mathbb{R}^{16}$  include  $\mathbf{p}_c$ ,  $\Theta$ , and  $\mathbf{q}_j$ .

$$\mathbf{H}(\mathbf{q})\ddot{\mathbf{q}} + \mathbf{C}(\mathbf{q}, \dot{\mathbf{q}}) = \mathbf{\Gamma} + \mathbf{J}_i(\mathbf{q})^\top \boldsymbol{\lambda}_i \quad (1)$$

where  $\mathbf{H} \in \mathbb{R}^{16 \times 16}$  is the mass-inertia matrix and  $\mathbf{C} \in \mathbb{R}^{22}$  is the joint-space bias force term.  $\mathbf{\Gamma} = [0_6; \boldsymbol{\tau}_j]$  represents the actuation in the generalized coordinate.  $\boldsymbol{\lambda}_i$  and  $\mathbf{J}_i$

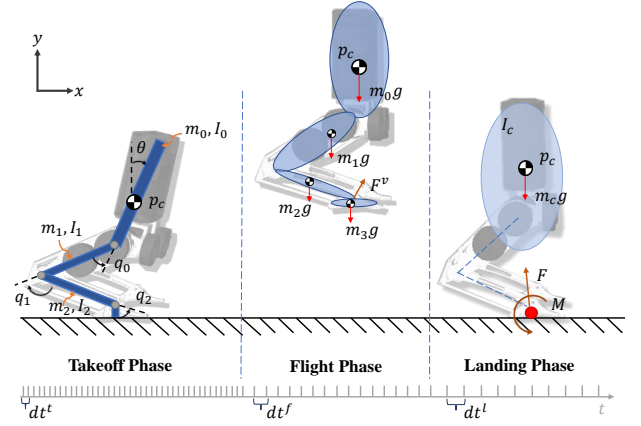


Fig. 4: Bipedal Dynamics Models. Adaptive dynamics model illustration during bipedal jumping in Adaptive-model TO: (1) Takeoff phase: 3-link inverted pendulum dynamics, (2) Flight phase: MRBD, (3) Landing phase: SRBD.

represent the external force applied to the system and its corresponding Jacobian matrix.

#### B. Adaptive-fidelity Dynamics Modeling

In the proposed Adaptive-model TO framework, we choose to use 3 different resolutions of dynamics models of bipedal robots for different phases of a jumping trajectory, illustrated in Fig. 4. By leveraging the adaptive models and adaptive sampling frequencies, the TO can be efficiently solved while retaining the necessary model resolutions for a hardware-realizable trajectory.

First, we classify the bipedal jumping trajectory into 3 phases, shown in Fig. 4: (1) takeoff phase, (2) flight phase, and (3) landing phase. The takeoff phase is measured from the beginning of the jumping motion until the robot's feet are off the ground. The flight phase is measured from when the robot becomes aerial until right before its touchdown and contact with the ground. The landing phase also only consists of when the robot's feet are in contact with the ground after touchdown and until the robot reaches the desired configuration.

##### 1) Takeoff Phase and 3-link Inverted Pendulum Model:

This phase presents the most challenging part of the jumping, needing to generate a good lift-off for the flight phase while satisfying many actuation constraints. To ensure the model accuracy and to leverage the whole-body motion for taking-off, we design the model of this in-contact phase with fine fidelity and fine sampling steps in optimization [25], [10]. Hence, we assume the biped stays in contact with the ground before flight and use a full dynamics model of a fixed-base 3-link inverted pendulum in 2D to represent the bipedal planar takeoff motion, as illustrated in Fig. 4. The fixed-base dynamics model has the advantage of lighter computation effort while still imposing virtual force constraints to represent ground reaction forces of a float-base model, which will be discussed in Section. III-C. Each pendulum link has physical properties representing the corresponding

biped link's mass and moment of inertia (MoI). The Euler-Lagrangian dynamics is as follows,

$$\mathbf{H}_{ip}(\mathbf{q}_{ip})\ddot{\mathbf{q}}_{ip} + \mathbf{C}_{ip}(\mathbf{q}_{ip}, \dot{\mathbf{q}}_{ip}) = \boldsymbol{\tau}_{ip} \quad (2)$$

where  $\mathbf{q}_{ip} = [q_0, q_1, q_2]^\top$  describes the 3-link inverted pendulum joint states.  $\boldsymbol{\tau}_{ip}$  represents the 3-link model joint torques.

2) *Flight Phase and MRBD*: In this phase, it is important to consider the dynamic effect of the leg links on the angular momentum of the whole body and let the TO determine where to place each link during the flight to result in a proper landing configuration. At the same time, a fine full-order dynamics model will not benefit much due to the minor adjustments of legs in the air. Hence, we use a multi-rigid-body dynamics model, in which each link's dynamic effect is simplified as external forces applied to the trunk CoM 2D location  $\mathbf{p}_c^{2D}$ . Note that we impose a virtual foot force  $\mathbf{F}^v$  in dynamics formulation, to capture the effect of joint torques during flight phase. The MRBD equations of motion are as follows,

$$m_0(\ddot{\mathbf{p}}_c^{2D} + \mathbf{g}) = \mathbf{F}^v + \sum_{n=1}^3 -m_n \mathbf{g} \quad (3)$$

$$\frac{d}{dt}(I_0 \dot{\theta}) = (\mathbf{p}_f - \mathbf{p}_c^{2D}) \times \mathbf{F}^v + \sum_{n=1}^3 (\mathbf{p}_n - \mathbf{p}_c^{2D}) \times -m_n \mathbf{g} \quad (4)$$

where  $m_n$  represents the mass of each link  $n$ ,  $n = 1, 2, 3$ ,  $I_0$  represents the MoI of the trunk link,  $\theta$  represents the robot's pitch angle,  $\mathbf{p}_n$  and  $\mathbf{p}_f$  are the CoM location of each link and foot location in the world frame, accessed by forward kinematics (FK) of joint angles,  $\text{FK}(\mathbf{q}_{ip})$ .

3) *Landing Phase and SRBD*: As many legged-jumping TO frameworks have omitted, we choose to design the TO to include a landing and balancing phase of the jumping motion to generate a recovery trajectory for real-time Adaptive-frequency MPC to follow. Force-based dynamics modeling is an effective approach in real-time control to allow soft impact [29]. In addition, to establish a unified control framework and synchronize with the modeling of biped in our MPC, we design the landing part of the adaptive model to become a single-rigid-body dynamics model, as described in detail in authors' prior work [30] and many other SRBD-based MPC on legged robots [31], [32]. The 2D EoM during landing is as follows,

$$m_0(\ddot{\mathbf{p}}_c^{2D} + \mathbf{g}) = \mathbf{F} \quad (5)$$

$$\frac{d}{dt}(I_c \dot{\theta}) = (\mathbf{p}_f - \mathbf{p}_c^{2D}) \times \mathbf{F} + M \quad (6)$$

where  $\mathbf{F}$  is the 2D ground reaction force at the contact point,  $M$  is the ground reaction moment in the x-y plane.

### C. Adaptive-model Trajectory Optimization

With the adaptive-fidelity models introduced, the following section will explain the details of the proposed Adaptive-model TO and its NLP formulation.

The Adaptive-model TO serves as a trajectory generator for bipedal jumping and landing motions. The information taken from the environment or specified by the users is

used as the inputs to the TO, in terms of jump distance, obstacle height, and desired landing location to describe the jumping tasks. The TO is carefully designed to reflect the model fidelity requirements at different jumping phases. The Adaptive-model TO is formulated as a direct collocation TO problem and is efficiently solved as an NLP problem with constraints reflecting its adaptive-model dynamics and sampling rates.

The optimization variables chosen in this TO are,

$$\mathbf{X} = [\mathbf{x}_c, \mathbf{q}_{ip}, \dot{\mathbf{q}}_{ip}, \boldsymbol{\tau}_{ip}, \mathbf{F}, M, dt^f, dt^l]^\top; \quad (7)$$

where  $dt^f$  is the flight phase step length and  $dt^l$  is the landing phase step length. We choose to let the optimization determine the lengths of sampling steps during each phase, to prevent hard constraints on  $dt$ , which may lead to the optimization solving with infeasible contact timings or heavier computation. Note that  $\mathbf{x}_c = [p_{c,x}, p_{c,y}, \theta, \dot{p}_{c,x}, \dot{p}_{c,y}, \dot{\theta}]^\top$  is the 2D representation of the robot trunk CoM states  $\mathbf{x}_c$ .

The formulation of the finite horizon optimization problem with  $N+1$  steps is as follows,

$$\min_{\mathbf{X}} \sum_{i=1}^{N+1} \left\| \mathbf{q}_{ip}[0] - \mathbf{q}_{ip}[i] \right\|_{\mathbf{Q}_0}^2 + \left\| \dot{\mathbf{q}}_{ip}[i] \right\|_{\mathbf{Q}_1}^2 + \left\| \boldsymbol{\tau}_{ip}[i] \right\|_{\mathbf{Q}_2}^2 \quad (8)$$

$$\text{s.t.} \quad \text{Joint angle: } \mathbf{q}_{min} \leq \mathbf{q}_{ip}[i] \leq \mathbf{q}_{max} \quad (9a)$$

$$\text{Joint speed: } \dot{\mathbf{q}}_{min} \leq \dot{\mathbf{q}}_{ip}[i] \leq \dot{\mathbf{q}}_{max} \quad (9b)$$

$$\text{Joint torque: } \boldsymbol{\tau}_{min} \leq \boldsymbol{\tau}_{ip}[i] \leq \boldsymbol{\tau}_{max} \quad (9c)$$

$$\text{Motor Max Power: } P_{motor}[i] \leq 400\text{W} \quad (9d)$$

$$\text{Initial Condition: } \mathbf{x}_c[0] = \mathbf{x}_c^{IC} \quad (9e)$$

$$\text{Final Condition: } \mathbf{x}_c[N+1] = \mathbf{x}_c^{FC} \quad (9f)$$

$$\text{Forward Kinematics: } \mathbf{x}_c[i] = \text{FK}(\mathbf{q}_{ip}[i], \dot{\mathbf{q}}_{ip}[i]) \quad (9g)$$

$$\text{Positive GRF: } 0 \leq \mathbf{F}[i] \quad (9h)$$

$$\text{Friction: } -\mu F_y[i] \leq F_x[i] \leq \mu F_y[i] \quad (9i)$$

$$\text{Line foot: } -l_h F_y[i] \leq M[i] \leq l_t F_y[i] \quad (9j)$$

---

**Takeoff Phase**  $i = 0 : N^t - 1$

$$\begin{aligned} \text{Dynamics (2): } \quad & \ddot{\mathbf{q}}_{ip}[i] = \mathbf{H}_{ip}^{-1}[i](-\mathbf{C}_{ip}[i] + \boldsymbol{\tau}_{ip}[i]) \\ & \dot{\mathbf{q}}_{ip}[i+1] = \dot{\mathbf{q}}_{ip}[i] + \dot{\mathbf{q}}_{ip}[i] dt^t \\ & \mathbf{q}_{ip}[i+1] = \mathbf{q}_{ip}[i] + \dot{\mathbf{q}}_{ip}[i] dt^t \end{aligned} \quad (10a)$$

$$\text{Support region: } -l_h \leq p_{rc,x}(\mathbf{q}_{ip}[i]) \leq l_t \quad (10b)$$

$$\text{Virtual GRFM: } [\mathbf{F}[i]; M[i]] = \mathbf{J}_c^\top \boldsymbol{\tau}_{ip}[i] \quad (10c)$$


---

**Flight Phase**  $i = N^t : N^t + N^f - 1$

$$\text{Dynamics (3-4): } \mathbf{x}_{ip}[i+1] = \mathbf{x}_{ip}[i] + \dot{\mathbf{x}}_{ip}[i] dt^f \quad (11a)$$

$$\text{Collision avoidance: } h_{terrain}[i] < p_{toe,y}(\mathbf{q}_{ip}[i]) \quad (11b)$$

$$\text{Minimal actuation: } |\mathbf{F}^v[i]| \leq 10\text{N} \quad (11c)$$

$$\text{Sampling rate: } 0 \leq dt^f \quad (11d)$$


---

**Landing Phase**  $i = N^t + N^f : N$

$$\text{Dynamics (5-6): } \mathbf{x}_{ip}[i+1] = \mathbf{x}_{ip}[i] + \dot{\mathbf{x}}_{ip}[i] dt^l \quad (12a)$$

$$\text{Sampling rate: } 0.02\text{s} \leq dt^l \leq 0.05\text{s} \quad (12b)$$

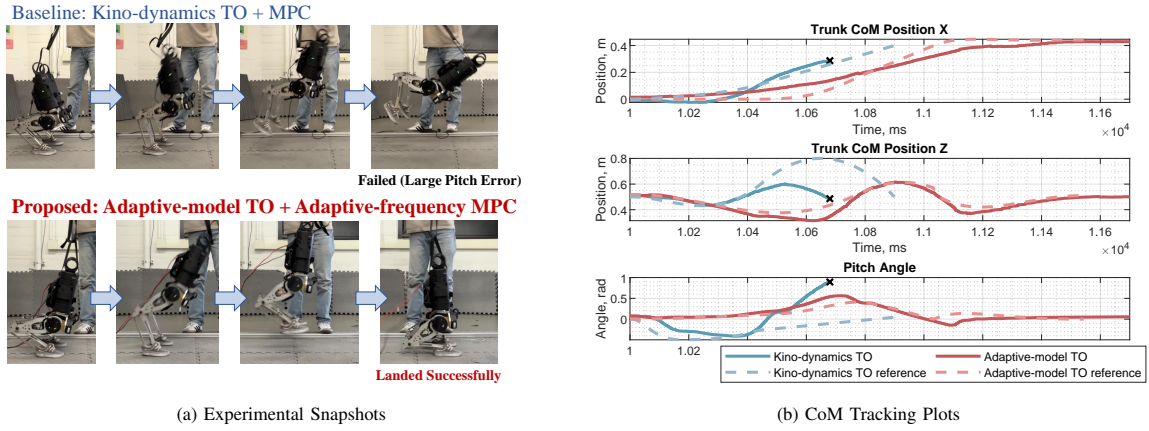


Fig. 5: **Comparing Adaptive-model TO with Kino-dynamics TO Results in Jumping Experiments.** In the baseline approach, we use a Kino-dynamics model in TO to solve for jumping trajectory over 0.4m distance and use SRBD-based MPC + joint PD control for real-time trajectory tracking. In the proposed Adaptive-model TO approach, the real-time control strategy is the combination of Adaptive-frequency MPC + joint PD control.

The objectives of the TO in (8) contain minimizing joint movement, joint speed, and joint torque during the entire jumping motion. The goal is to generate a fluent jump with minimal actuation efforts.  $Q_0$ ,  $Q_1$ , and  $Q_2$  are objective weighting matrices. The NLP is subjected to several constraints. (9a-9c) describe the joint kinematics and actuation limits. (9d) describes the Unitree A1 motor power constraints based on its efficiency and wattage limit, which is an effective approach to ensure actuation awareness for hardware experiments [10], [14]. (9e-9f) describes the initial and final conditions of the robot, based on the terrain setup and user commands. We use FK described in (9g) to bridge the joint space states  $q_{ip}$  and robot trunk CoM states  $x_c$  and their discrete dynamics representations in adaptive models. (9h-9i) ensure the ground reaction forces are always positive and respect friction constraints. (9j) describes the contact wrench cone constraint of line-foot [33].

Additional constraints are given and phase-specific, besides adaptive dynamics modeling. In (10c), we impose a virtual ground reaction forces  $F$  and moment  $M$  from joint torques and virtual contact Jacobian in the 3-link dynamics model to amplify the 3-link fix-base model to behave close to a float-base model when in contact with the ground. (10b) ensures the CoM of the entire robot,  $p_{rc}$  stays within the support region, formed by the toe and heel length,  $l_t, l_h$ . During flight phase, (11b) enforces the foot height of the robot  $p_{toe,y}$  always above the terrain. (11c) allows for small virtual Cartesian foot forces (translated to joint torque actuations) to be applied to the dynamics, which enables the TO to adjust the robot's feet and combined MoI during flight for better landing configuration.

#### D. Adaptive-frequency MPC

Once the Adaptive-model TO generates an optimal jumping trajectory, the Adaptive-frequency MPC will work in conjunction with joint PD control to track the reference trajectories  $x_c^{ref}$  and  $q_j^{ref}$ , which are mapped directly from optimization result  $X$ . In addition, the adaptive-frequency MPC takes in the planned contact sequence and optimal

variable sampling frequencies  $dt$  of each phase, to ensure the synchronization of sampling frequencies between TO and MPC and fully leverage the trajectory resolutions.

Adaptive-frequency MPC leverages the linearized SRBD of bipedal robot HECTOR, with the assumption of negligible effect of leg movement during landing control. The dynamics formulation follows the single rigid-body modeling in the author's prior work [26], a 3D extension of (5-6). We choose to include gravity  $g$  in the optimization variable  $x = [x_c; g]$  to linearize the dynamics and form  $\dot{x}(t) = \hat{A}_c x + \hat{B}_c u$ , where  $\hat{A}_c \in \mathbb{R}^{15 \times 15}$  and  $\hat{B}_c \in \mathbb{R}^{15 \times 10}$  are continuous-time state-space dynamics matrices. Translating it to discrete-time form at  $i$ th step with variable  $dt[i]$ :

$$x[i+1] = \hat{A}_d[i]x[i] + \hat{B}_d[i]u[i] \quad (13)$$

$$\hat{A}_d = I_{15} + \hat{A}_c \cdot dt[i], \quad \hat{B}_d = \hat{B}_c \cdot dt[i] \quad (14)$$

The control input  $u$  includes the 3D ground reaction forces and moments of both foot,  $u = [F_0; F_1; M_0; M_1]$ . The formulation of the optimization problem with finite horizon  $k$  can be written in the following form,

$$\min_{x,u} \sum_{i=0}^k \left\| x[i] - x^{ref}[i] \right\|_{R_0}^2 + \left\| u[i] \right\|_{R_1}^2 \quad (15)$$

s.t.

$$\text{Dynamics: } x[i+1] = \hat{A}_d[i]x[i] + \hat{B}_d[i]u[i] \quad (16a)$$

$$\text{Friction pyramid of foot } n: \begin{aligned} -\mu F_{n,z}[i] &\leq F_{n,x}[i] \leq \mu F_{n,z}[i] \\ -\mu F_{n,z}[i] &\leq F_{n,y}[i] \leq \mu F_{n,z}[i] \end{aligned} \quad (16b)$$

$$\text{Force limit: } 0 \leq F_{n,z}[i] \leq F_{max} \quad (16c)$$

$$\text{Moment X: } \mathcal{B}M_x[i] = 0 \quad (16d)$$

$$\text{Line foot: } -l_h F_z[i] \leq M_y[i] \leq l_t F_z[i] \quad (16e)$$

The objective of the problem is to drive state  $x$  close to the Adaptive-model TO reference and minimize control input  $u$ . These objectives are weighted by diagonal matrices  $R_0 \in \mathbb{R}^{15 \times 15}$  and  $R_1 \in \mathbb{R}^{10 \times 10}$ . (16d) enforces foot moment in the x-direction is always zeros in the robot's body frame, as discussed in [30].

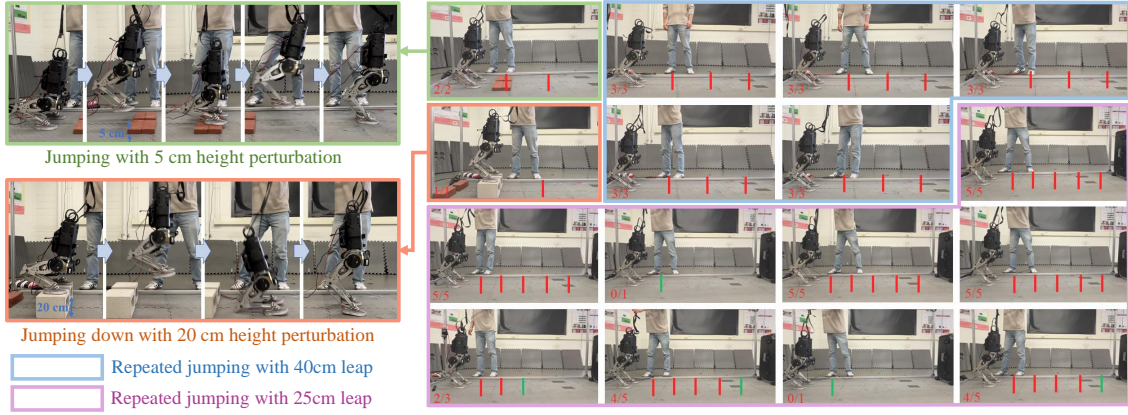


Fig. 6: **Jumping Repeatability Experiment.** On the left, the highlighted snapshots are experiments with perturbations to the terrain. The rest of the snapshots on the right are categorized into 25cm and 40cm leaps. Each snapshot represents a repeated jumping trial. The red markers indicate successful jumps and the green markers indicate failed ones. The successful jumps over total jumps in each trial are displayed at the corner of the snapshot, yielding 90% success rate based on the above experiments.

TABLE I: Experiment Parameters

$Q_0 = 0.1$	$N^t = 70, dt^t = 0.01s$
$Q_1 = 0.5$	$N^f = 30$
$Q_2 = 0.01$	$N^l = 30$
$\mu = 0.5$	$k = 10$
$R_0 = \text{diag}([300 \ 300 \ 400 \ 150 \ 200 \ 150 \ 1 \ 1 \ 1 \ 1 \ 10 \ 0])$	
$R_1 = \text{diag}([1 \ 1 \ 1 \ 1 \ 1 \ 1 \ 1 \ 1 \ 1 \ 1 \ 1] \cdot 10^{-6})$	
$K_p = \text{diag}([150 \ 150 \ 150 \ 150 \ 100])$	
$K_d = \text{diag}([2 \ 2 \ 2 \ 2 \ 1])$	

### E. Real-time Jumping Control

The real-time jumping control consists of both Adaptive-frequency MPC for tracking CoM trajectory and joint-PD control for tracking the joint trajectory simultaneously. The joint torque command is computed as,

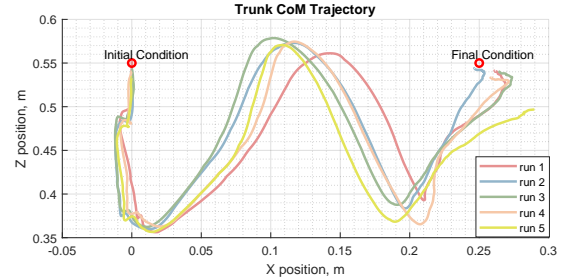
$$\tau_j = K_p(\dot{q}_j^{ref} - \dot{q}_j) + K_d(\ddot{q}_j^{ref} - \ddot{q}_j) + J_c^T u \quad (17)$$

where  $J_c$  is the contact points' world frame Jacobian matrix.

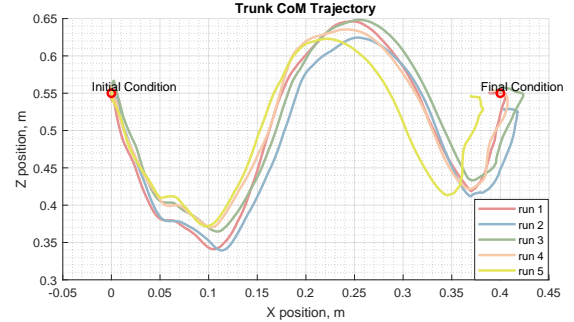
To realize dynamic continuous jumping behaviors, it is important to synergize the Adaptive-model TO and Adaptive-frequency MPC together, by leveraging the variable frequency  $dt$  and forming a reasonable preview trajectory for each jumping phase. In addition, we connect each jump's end configuration with the next jump's initial configuration by MPC and guide the robot to prepare for the following jump [34]. Compared to single jumping motions, in continuous jumping, after the landing of each jump, instead of raising its CoM height to nominal height, the robot immediately takes off at the lowered height to leverage the conserved energy during impact. The adaptive-frequency MPC bridges the two jumps by adapting its sampling frequency at the prediction horizon and connecting the variable-frequency reference trajectories together seamlessly.

## IV. RESULTS

This section presents the hardware results of the proposed Adaptive-model Optimization framework in bipedal jumping, including comparison with other popular approaches,



(a) 25 cm leap experiments trajectory overlay



(b) 40 cm leap experiments trajectory overlay

Fig. 7: **Jumping Trajectories Overlay** CoM trajectories of only 5 runs of each category are overlaid.

robustness in balancing with MPC after free fall, repeatability experiment with 53 jumping experiments, and continuous jumping over platforms with gaps and height perturbations. It is encouraged to watch the supplementary videos for better visualization of the results<sup>1</sup>.

### A. Experiment Setup

We use MATLAB to generate the reference trajectories of jumping tasks. The NLP problem is setup and solved with CasADi toolbox [35] and IPOPT solver. The proposed Adaptive-model TO, with 20 randomized problem setups (i.e., initial conditions and end conditions), results in an

<sup>1</sup>Hardware experiment video: <https://youtu.be/EQFgdbFYKvs>

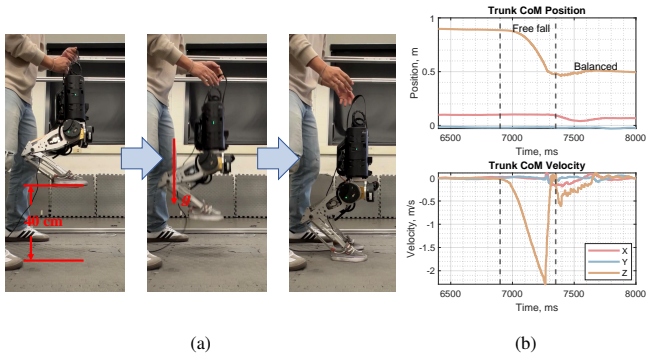


Fig. 8: **Balancing after 0.4 m Freefall.** (a). Experimental snapshots. (b). CoM position and velocity plots.

average solve time of 7.5 s on a Ubuntu 20.04 desktop, equipped with AMD 5600X CPU clocked at 4.2 GHz. On the hardware, the real-time MPC is solved as a quadratic programming (QP) problem via `qpOASES` solver in C++. The detailed parameters are shown in Table. I.

### B. Comparison of Approaches in Bipedal Jumping

Firstly, we present the comparison of our proposed Adaptive-model TO approach to the Kino-dynamics TO approach in bipedal jumping, shown in Fig. 5. In both experiments, we generate 40 cm jumping TO, and the trajectories are tracked by MPC and joint PD control. It is observed that, in the Kino-dynamic TO experiment, the error accumulates very fast after taking off, especially due to the lack of consideration of the actuation and the effect of leg dynamics during the takeoff phase, resulting in a very large pitch angle during flight. On the other hand, with the proposed Adaptive-model TO approach and Adaptive-frequency MPC, the trajectory tracking is much smoother. The robot CoM follows the desired path after taking off and reaches a good landing configuration for balancing and recovery after impact.

### C. Jumping Repeatability

To validate the repeatability of the jumping behaviors with the proposed framework, we run 53 jumps, which include (1) 18 trials of jumps with a 40 cm distance target and (2) 35 trials of jumps with a 25 cm distance target. Fig. 6 showcases these experiments, each red marker represents a successful jump, green marker represents a failed jump. 3 of the jumps in category (1) are perturbed by the initial and end terrain heights, up to 20 cm. As a result, 48 out of the 53 attempts succeed and balance well after jumping. 5 of each jumping trajectories are overlaid in Fig. 7a and 7b to showcase the consistency of performance and trajectory tracking with our control framework.

### D. Landing Robustness

A successful jump cannot omit the importance of its landing. In this work, we leverage the Adaptive-frequency MPC and SRBD for impact absorption and recovery after

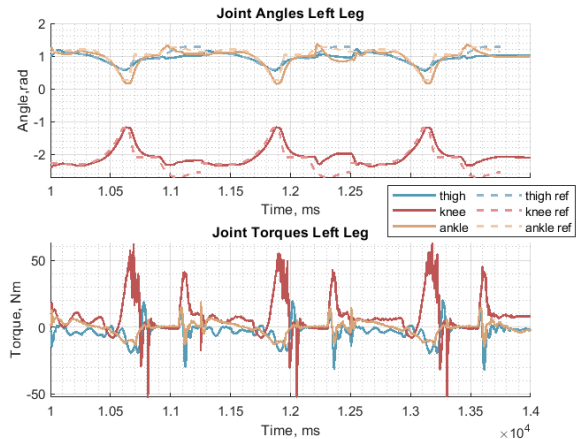


Fig. 9: **Continuous Jumping over Discrete Terrain Experiment Joint Plots.** Left leg joint position tracking and joint torque plots. Note that the hip yaw and hip roll joints are omitted for comparison in this plot due to sagittal motion.

landing. We verify the robustness of the landing control by manually dropping the robot from a height of 40 cm foot clearance off the ground (57% of robot height), shown in Fig. 8. The robot can effectively absorb the impact and high z-direction velocity after freefall and balance immediately.

### E. Continuous Jumping over Discrete Terrain

In addition to single jumps, we have successfully demonstrated the effectiveness of our control method in dynamic continuous jumps. Fig. 1 shows the motion snapshots of 3 continuous jumps over wooden boxes to mimic terrain with discontinuities and large gaps of up to 20 cm. The boxes also have increasing heights, each by 5 cm. With the proposed Adaptive-model Optimization methods, the robot is able to comfortably jump over these boxes in less than 6 seconds. The joint tracking and torque plots are shown in Fig. 9, demonstrating good tracking performance while staying within actuation limits.

## V. CONCLUSIONS

In conclusion, we propose an Adaptive-model Optimization framework to effectively address the problem of dynamic continuous jumping on bipedal robots. The proposed Adaptive-model Trajectory Optimization consists of adaptive dynamics modeling with varied model fidelity and sampling frequency during different jumping phases. We pair this TO framework with a single-rigid-body model based Adaptive-frequency MPC to capture the synchronization of sampling rates between TO and online MPC. We validated the proposed approach in hardware with HECTOR bipedal robot, realizing dynamic jumping behaviors covering a jumping distance of up to 40 cm. We verify the repeatability and robustness of the jumping motions through 53 trials of jumping and achieve a 90% success rate. The proposed control framework has also allowed the robot to jump continuously and dynamically over 3 boxes with gaps up to 20 cm in less than 6 seconds.

## VI. ACKNOWLEDGEMENT

The authors would like to extend special thanks to Junchao Ma and Lokesh Krishna for their hardware and experimental support.

## REFERENCES

- [1] Q. Nguyen, A. Agrawal, W. Martin, H. Geyer, and K. Sreenath, "Dynamic bipedal locomotion over stochastic discrete terrain," *The International Journal of Robotics Research*, vol. 37, no. 13-14, pp. 1537–1553, 2018.
- [2] D. Kim, S. J. Jorgensen, J. Lee, J. Ahn, J. Luo, and L. Sentis, "Dynamic locomotion for passive-ankle biped robots and humanoids using whole-body locomotion control," *The International Journal of Robotics Research*, vol. 39, no. 8, pp. 936–956, 2020.
- [3] Z. Li, X. Cheng, X. B. Peng, P. Abbeel, S. Levine, G. Berseth, and K. Sreenath, "Reinforcement learning for robust parameterized locomotion control of bipedal robots," in *2021 IEEE International Conference on Robotics and Automation (ICRA)*, pp. 2811–2817, IEEE, 2021.
- [4] G. Gibson, O. Dosunmu-Ogunbi, Y. Gong, and J. Grizzle, "Terrain-adaptive, alip-based bipedal locomotion controller via model predictive control and virtual constraints," in *2022 IEEE/RSJ International Conference on Intelligent Robots and Systems (IROS)*, pp. 6724–6731, IEEE, 2022.
- [5] Z. Gu, Y. Zhao, Y. Chen, R. Guo, J. K. Leestma, G. S. Sawicki, and Y. Zhao, "Robust-locomotion-by-logic: Perturbation-resilient bipedal locomotion via signal temporal logic guided model predictive control," *arXiv preprint arXiv:2403.15993*, 2024.
- [6] M. Vukobratović, B. Borovac, and D. Šurdilović, "Zero moment point-proper interpretation and new applications," in *Int. Conf. on Humanoid Robots*, pp. 237–244, 2001.
- [7] C. L. Vaughan, "Theories of bipedal walking: an odyssey," *Journal of biomechanics*, vol. 36, no. 4, pp. 513–523, 2003.
- [8] <https://www.youtube.com/watch?v=tF4DML7FIWk>, "Atlas | partner in parkour,"
- [9] <https://www.youtube.com/watch?v=V1LyWsiTgms>, "Unitree h1 the world's first full-size motor drive humanoid robot flips on ground,"
- [10] Q. Nguyen, M. J. Powell, B. Katz, J. Di Carlo, and S. Kim, "Optimized jumping on the mit cheetah 3 robot," in *2019 International Conference on Robotics and Automation (ICRA)*, pp. 7448–7454, IEEE, 2019.
- [11] M. Chignoli, S. Morozov, and S. Kim, "Rapid and reliable quadruped motion planning with omnidirectional jumping," in *2022 International Conference on Robotics and Automation (ICRA)*, pp. 6621–6627, IEEE, 2022.
- [12] Y. Ding, C. Li, and H.-W. Park, "Kinodynamic motion planning for multi-legged robot jumping via mixed-integer convex program," in *2020 IEEE/RSJ International Conference on Intelligent Robots and Systems (IROS)*, pp. 3998–4005, IEEE, 2020.
- [13] G. Bellegarda, M. Shafiee, M. E. Özberk, and A. Ijspeert, "Quadruped-frog: Rapid online optimization of continuous quadruped jumping," *arXiv preprint arXiv:2403.06954*, 2024.
- [14] M. Chignoli, D. Kim, E. Stanger-Jones, and S. Kim, "The mit humanoid robot: Design, motion planning, and control for acrobatic behaviors," in *2020 IEEE-RAS 20th International Conference on Humanoid Robots (Humanoids)*, pp. 1–8, IEEE, 2021.
- [15] P. M. Wensing and D. E. Orin, "Generation of dynamic humanoid behaviors through task-space control with conic optimization," in *2013 IEEE International Conference on Robotics and Automation*, pp. 3103–3109, IEEE, 2013.
- [16] X. Xiong and A. D. Ames, "Bipedal hopping: Reduced-order model embedding via optimization-based control," in *2018 IEEE/RSJ International Conference on Intelligent Robots and Systems (IROS)*, pp. 3821–3828, IEEE, 2018.
- [17] J. Zhang, J. Shen, Y. Liu, and D. Hong, "Design of a jumping control framework with heuristic landing for bipedal robots," in *2023 IEEE/RSJ International Conference on Intelligent Robots and Systems (IROS)*, pp. 8502–8509, IEEE, 2023.
- [18] W. Yang and M. Posa, "Impact invariant control with applications to bipedal locomotion," in *2021 IEEE/RSJ International Conference on Intelligent Robots and Systems (IROS)*, pp. 5151–5158, IEEE, 2021.
- [19] D. E. Orin, A. Goswami, and S.-H. Lee, "Centroidal dynamics of a humanoid robot," *Autonomous robots*, vol. 35, no. 2, pp. 161–176, 2013.
- [20] A. Herzog, S. Schaal, and L. Righetti, "Structured contact force optimization for kino-dynamic motion generation," in *2016 IEEE/RSJ International Conference on Intelligent Robots and Systems (IROS)*, pp. 2703–2710, IEEE, 2016.
- [21] M. Posa, C. Cantu, and R. Tedrake, "A direct method for trajectory optimization of rigid bodies through contact," *The International Journal of Robotics Research*, vol. 33, no. 1, pp. 69–81, 2014.
- [22] C. Nguyen and Q. Nguyen, "Contact-timing and trajectory optimization for 3d jumping on quadruped robots," in *2022 IEEE/RSJ international conference on intelligent robots and systems (IROS)*, pp. 11994–11999, IEEE, 2022.
- [23] H. Li, R. J. Frei, and P. M. Wensing, "Model hierarchy predictive control of robotic systems," *IEEE Robotics and Automation Letters*, vol. 6, no. 2, pp. 3373–3380, 2021.
- [24] H. Li and P. M. Wensing, "Cafe-mpc: A cascaded-fidelity model predictive control framework with tuning-free whole-body control," *arXiv preprint arXiv:2403.03995*, 2024.
- [25] N. Csomay-Shanklin, V. D. Dorobantu, and A. D. Ames, "Nonlinear model predictive control of a 3d hopping robot: Leveraging lie group integrators for dynamically stable behaviors," in *2023 IEEE International Conference on Robotics and Automation (ICRA)*, pp. 12106–12112, IEEE, 2023.
- [26] J. Li and Q. Nguyen, "Dynamic walking of bipedal robots on uneven stepping stones via adaptive-frequency MPC," *IEEE Control Systems Letters*, 2023.
- [27] J. Li, J. Ma, O. Kolt, M. Shah, and Q. Nguyen, "Dynamic locomotion on hector: Humanoid for enhanced control and open-source research," *arXiv preprint arXiv:2312.11868*, 2023.
- [28] DRCL-USC, "[https://github.com/DRCL-USC/Hector\\_Simulation](https://github.com/DRCL-USC/Hector_Simulation)."
- [29] P. M. Wensing, A. Wang, S. Seok, D. Otten, J. Lang, and S. Kim, "Proprioceptive actuator design in the mit cheetah: Impact mitigation and high-bandwidth physical interaction for dynamic legged robots," *Ieee transactions on robotics*, vol. 33, no. 3, pp. 509–522, 2017.
- [30] J. Li and Q. Nguyen, "Force-and-moment-based model predictive control for achieving highly dynamic locomotion on bipedal robots," in *2021 60th IEEE Conference on Decision and Control (CDC)*, pp. 1024–1030, IEEE, 2021.
- [31] J. Di Carlo, P. M. Wensing, B. Katz, G. Bleidt, and S. Kim, "Dynamic locomotion in the mit cheetah 3 through convex model-predictive control," in *2018 IEEE/RSJ International Conference on Intelligent Robots and Systems (IROS)*, pp. 1–9, IEEE, 2018.
- [32] Y. Ding, C. Khazoom, M. Chignoli, and S. Kim, "Orientation-aware model predictive control with footstep adaptation for dynamic humanoid walking," in *2022 IEEE-RAS 21st International Conference on Humanoid Robots (Humanoids)*, pp. 299–305, IEEE, 2022.
- [33] S. Caron, Q.-C. Pham, and Y. Nakamura, "Stability of surface contacts for humanoid robots: Closed-form formulae of the contact wrench cone for rectangular support areas," in *2015 IEEE International Conference on Robotics and Automation (ICRA)*, pp. 5107–5112, IEEE, 2015.
- [34] C. Nguyen, L. Bao, and Q. Nguyen, "Continuous jumping for legged robots on stepping stones via trajectory optimization and model predictive control," in *2022 IEEE 61st Conference on Decision and Control (CDC)*, pp. 93–99, IEEE, 2022.
- [35] J. A. E. Andersson, J. Gillis, G. Horn, J. B. Rawlings, and M. Diehl, "CasADI – A software framework for nonlinear optimization and optimal control," *Mathematical Programming Computation*, vol. 11, no. 1, pp. 1–36, 2019.